Substrate coherency driven octahedral rotations in perovskite oxide films

James M. Rondinelli[*,†] and Nicola A. Spaldin
Materials Department, University of California, Santa Barbara, California 93106, USA
(Received 2 August 2010; published 2 September 2010)

We perform first-principles density-functional calculations to explore the role of substrate proximity effects on the octahedral rotation patterns in perovskite oxide superlattices. With cubic perovskite $SrFeO_3$ as our model film and tetragonal $SrTiO_3$ as the substrate, we show that in most cases the substrate octahedral rotation patterns propagate into the film across the heterointerface. We also identify elastic boundary conditions for which the enforced structural coherence induces atomic displacement patterns that are not found in the bulk phase diagram of either individual constituent. We suggest that such substrate coherency-induced octahedral texturing of thin film oxides is a promising approach for tuning the electronic structure of functional oxide thin films.

DOI: 10.1103/PhysRevB.82.113402 PACS number(s): 68.65.−k, 71.15.Mb, 71.30.+h

The use of substrate-induced biaxial strain to modify the properties of epitaxial thin films has been demonstrated for a wide range of phenomena and materials, including mobility in semiconductors, Curie temperatures in ferromagnets and ferroelectric polarizations in complex oxides.[1] While the main effect of strain in strongly covalently bonded materials such as semiconductors is to change the bond lengths, the flexible corner-sharing networks of oxygen polyhedra in complex oxides provide additional routes for accommodating substrate-induced changes in lattice parameters. Established mechanisms include modifications of the oxygen polyhedral tilt patterns, and the formation of twin (change in orientation of long and short axes) or antiphase (variation in phase of polyhedral rotations) domains.

Recently it is been suggested that, in addition to changing the lattice parameter of a complex oxide film, the presence of a heterointerface could alter the relative stability of polyhedral tilting patterns in both the film and substrate through proximity effects.[2–5] While theoretical studies have shown that strain-induced competition between polyhedral rotation modes and other lattice distortions is crucial in determining the functional properties of complex oxides,[6–11] very little is known about the extent to which substrate proximity modifies polyhedral tilt patterns. This is in part due to difficulties in obtaining high precision measurements of oxygen positions in superlattice and thin film interfaces.[12,13] In this Brief Report, we use density-functional theory (DFT) to calculate explicitly how a substrate's structural distortions affect the atomic structure and properties of a coherent film.

We take perovskite-structured $SrFeO_3/SrTiO_3$ as our model system, chosen for its continuous A-site sublattice, absence of polar discontinuity, and simple oxygen octahedral tilt patterns: $SrFeO_3$ has the ideal cubic $Pm\bar{3}m$ perovskite structure down to the lowest temperature studied (4 K),[14] and the ground state $I4/mcm$ phase of $SrTiO_3$ (which is a widely used substrate) has a single octahedral instability with respect to the cubic phase[15] that condenses below ~105 K. First, we investigate the effect of heterostructure periodicity in symmetric $(SrTiO_3)_n/(SrFeO_3)_n$, $n=1\ldots5$, and asymmetric $(SrTiO_3)_n/(SrFeO_3)_m$, $n=1\ldots3, m=1\ldots3$ superlattices. We find that the octahedral rotations from the $SrTiO_3$ substrate propagate into the first two interfacial $SrFeO_3$ layers to induce octahedral rotations where none exist in the bulk material; for highly confined ferrate layers additional electronically driven lattice instabilities occur that are not observed in bulk $SrFeO_3$. Then we show that these octahedral and electronic lattice instabilities cannot be induced in $SrFeO_3$ using biaxial strain alone, indicating that substrate coherency and confinement play a critical role in determining the heterointerface atomic structure.

Our DFT calculations are performed within the local spin-density approximation+Hubbard U (LSDA+U) method using the Vienna *ab initio* simulation package (VASP),[16,17] with the Dudarev method[18] for the Hubbard correction to the LSDA exchange-correlation functional. Consistent with earlier first-principles calculations,[19] we use an effective U parameter of 6 eV on the Fe d orbitals and impose ferromagnetic spin order in the $SrFeO_3$. Complete details of our calculations are reported elsewhere.[20]

We first calculate how freezing in the antiferrodistortive (AFD) $a^0a^0c^-$ octahedral tilt pattern of the low-temperature phase of $SrTiO_3$ (Ref. 21) affects the total energies of the two bulk materials which comprise the superlattices. Figure 1(a) shows the calculated total energies as a function of increasing amplitude of octahedral rotation angle θ, referenced to the unrotated states at the L(S)DA equilibrium lattice parameters. As expected for bulk $SrFeO_3$, we find that the cubic perovskite structure is stable with respect to the octahedral rotation mode. In contrast, the $a^0a^0c^-$ tilt pattern is energy lowering for tetragonal $SrTiO_3$, consistent with the low-temperature experimental structure.[30]

We next explore whether heterostructuring $SrFeO_3$ layers with $SrTiO_3$ in different period superlattices induces AFD FeO_6 instabilities in the ferrate layers. We examine symmetric and asymmetric superlattices, by stacking (n,m) five-atom perovskite cells along the c-axis, with the in-plane periodicity increased to be commensurate with the AFD rotations. We keep the in-plane lattice constant fixed to the LDA equilibrium value of 3.86 Å to simulate epitaxial growth on tetragonal $SrTiO_3$ [$SrFeO_3$ is under a L(S)DA theoretical +1.75% biaxial strain]. The out-of-plane lattice constant of each superlattice is then fully relaxed.

We first uniformly introduce the same octahedral rotation pattern as before into each layer of superlattice. The evolution in the total energy for the asymmetric (n,m) and sym-

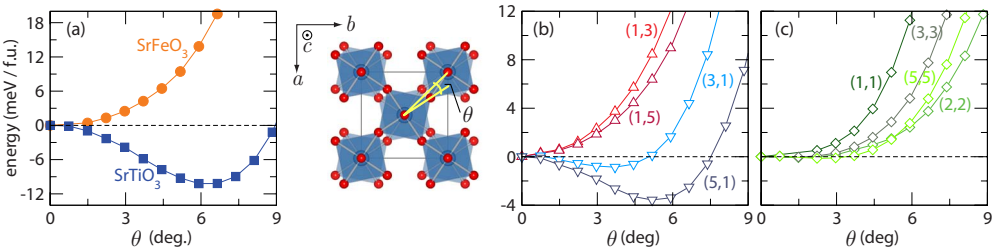

FIG. 1. (Color online) Energy versus rotation angle θ of the $a^0a^0c^-$ octahedral tilt for cubic $SrFeO_3$ and tetragonal $SrTiO_3$ (a). The same mode homogeneously frozen into (b) asymmetric $(SrTiO_3)_n/(SrFeO_3)_m$ and (c) symmetric superlattices (right).

metric (n,n) superlattices with increasing magnitude of θ is shown in Figs. 1(b) and 1(c). For the asymmetric superlattices we find that when $SrTiO_3$ comprises the majority of the superlattice, a homogeneous rotation of all octahedra is favored over the unrotated configuration. In contrast, the symmetric superlattices, and those with a greater fraction of $SrFeO_3$ layers are weakly, if at all, susceptible to the same rotational modes.

We next remove the artificial homogeneity constraint on the octahedral rotations and allow full relaxation of the oxygen positions in each layer within the symmetry of the $a^0a^0c^-$ tilt pattern. We initialize the oxygen positions in each superlattice to configurations corresponding to the energy well minima shown in Fig. 1. (For homogeneous rotations that were found to be stable, we start with $\theta=2°$.) The results of the structural relaxation are shown in Fig. 2, where we plot the layer-by-layer resolved rotations θ about the c axis for the different period superlattices. We find that in all cases, the octahedral rotations remain antiferrodistortive and that the $SrTiO_3$ substrate exhibits the $a^0a^0c^-$ tilt pattern. Interestingly, AFD octahedral rotations are induced in the interfacial $SrFeO_3$ layers, with the magnitude of the octahedral rotations decaying exponentially from the interface into the center of the $SrFeO_3$ slab. The layers in the center of each slab are close to their respective bulk calculated values, indicated by the broken lines, although the highly asymmetric (5,1) superlattice shows a 9.3% enhancement in θ at the center of the $SrTiO_3$ slab.

We next fully relax the atomic structure of each superlattice by removing the symmetry constraint imposed by the $a^0a^0c^-$ octahedral tilt pattern. The asymmetric superlattices in which $SrFeO_3$ is the majority component do not show any considerable changes in the atomic displacements: there is only a small decrease in the magnitude of the $a^0a^0c^-$ octahedral tilt at the interface due to small changes in the apical cation-oxygen bond lengths. We also found similar minor changes in the atomic structure for the symmetric superlattices (n,n) with $n \geq 2$. Therefore our earlier conclusion that only the first two ferrate interface unit cells are modified by the octahedral rotations found in the substrate remains for these cases.

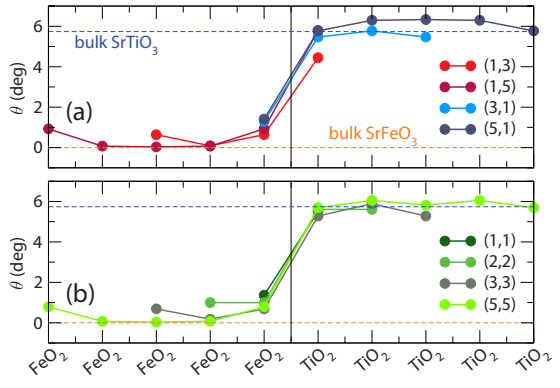

FIG. 2. (Color online) The layer-by-layer resolved octahedral rotation angles (θ) for the asymmetric (a) and symmetric (b) superlattices. The magnitude of the $SrTiO_3$ AFD octahedral rotations rapidly decreases into the $SrFeO_3$ interfacial layers.

Drastically different behavior is found, however, for superlattices with single unit cells of $SrFeO_3$: in the (1,1), (3,1), and (5,1) superlattices we find that, in addition to the original octahedral rotation pattern, the FeO_6 octahedra also exhibit Fe–O bond length distortions associated with electronic instabilities. In each case, either a Jahn-Teller (JT) distortion, which produces two short and two long equatorial Fe–O bonds, or a "breathing" distortion that makes a uniform dilation and contraction of the Fe–O bonds is found to be stable. Note that, for the single ferrate layer heterostructures, we obtain JT- and breathing-distorted FeO_6 octahedra even when we disable the oxygen octahedral rotations in our calculations. This indicates that these electronic instabilities are the consequence of the quantum confinement of the ferrate layer, which increases the susceptibility to electron localization and in turn enhances orbital degeneracy-lifting instabilities.[20] In the unrotated case, the energies of the JT- and breathing-distorted structures are energetically equivalent within the resolution of our DFT calculations.

While the JT- and breathing distortions are not induced by the octahedral rotations, when both rotations and JT- or breathing distortions are allowed, we are able to resolve distinct ground states, in which the octahedral rotations cooperate with a specific electronic instability. In the (3,1) superlattice, for example, the ground state consists of a large Jahn-Teller bond length distortion of 0.05 Å, in combination with a completely different octahedral rotation pattern—the well-known perovskite $a^-a^-c^+$ $GdFeO_3$ tilt pattern—that does not occur in either parent compound. If we instead enforce the usual $a^0a^0c^-$ tilt pattern of $SrTiO_3$, the superlattice exhibits a breathing distortion with Fe–O bond length differences of 6.6% between the two inequivalent FeO_6 octahedral sites.

We now check whether our finding of octahedral rotations within the $SrFeO_3$ interfacial layers can be reproduced using strain alone, or whether it requires substrate coherency. To explore the interaction between strain and the octahedral ro-

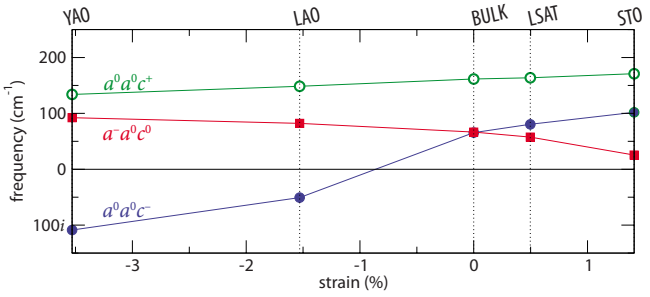

FIG. 3. (Color online) The effect of bi-axial strain on the mode stiffness of the rotational patterns in homogeneously strained [001]-orientated $SrFeO_3$ films. The out-of-plane lattice constant is chosen to conserve the experimental $SrFeO_3$ volume after fixing the in-plane lattice parameters to match the following substrates: $SrTiO_3$ (STO), LSAT=$(LaAlO_3)_{0.3}(Sr_2AlTaO_6)_{0.7}$, $LaAlO_3$ (LAO), and $YaAlO_3$ (YAO).

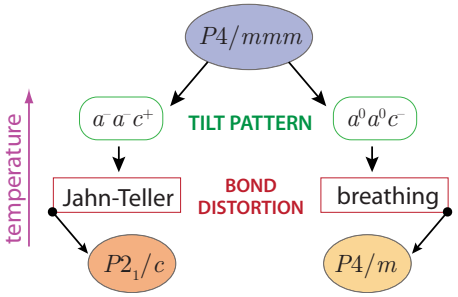

FIG. 4. (Color online) Illustration of how the same high symmetry reference superlattice can support either the electronically driven Jahn-Teller or breathing distortions by the condensation of different symmetry octahedral modes with temperature in the ferrate/titanate superlattices. The choice of a substrate based on the octahedral rotational properties may substitute for temperature to control such phases.

tations on the $SrFeO_3$ layers we remove the $SrTiO_3$ substrate from our calculations and simulate homoepitaxially strained $SrFeO_3$, with the bi-axial constraint imposed by enforcing equal in-plane lattice parameters. In addition to the ground state $a^0a^0c^-$ tilt pattern, we also examine the strain dependence of the in-phase $a^0a^0c^+$ rotation about the c-axis, the $a^-a^0c^0$ AFD tilt pattern about the a axis that lies in the epitaxial plane, and the Jahn-Teller and breathing distortions. Note that similar studies were performed previously for $SrTiO_3$;[22,23] we do not repeat those calculations here since our $SrTiO_3$ substrates are strain free.

In Fig. 3, we plot the calculated mode frequencies of the octahedral rotational patterns for a range of strain values corresponding to typical substrates. Real frequencies indicate that the cubic lattice is stable and that the mode does not spontaneously condense. Importantly, we find that all the frequencies are real for strain corresponding to coherency on $SrTiO_3$, indicating that the rotations in our $SrFeO_3/SrTiO_3$ heterostructures require the actual presence of the heterointerface, not only its associated strain. Under $>1\%$ compressive strain, we find an unstable $a^0a^0c^-$ rotation which has been reported previously for the case of $LaAlO_3$ (Ref. 24) and provides a low-energy route to reducing the in-plane lattice parameters without significantly shortening the bond lengths. The $a^-a^0c^0$ AFD tilt also softens with increasing tensile strain to accommodate the reduction in the out-of-plane lattice constant as the in-plane lattice parameters are elongated. We find that the in-phase $a^0a^0c^+$ tilt, however, is least sensitive to strain[31] and the Jahn-Teller and breathing distortions (data not shown) are disfavored for all strain states.

Finally, since we define strain relative to the LSDA equilibrium volumes in our calculations, we examine the dependence of the $SrFeO_3$ lattice instabilities on unit cell volume. We find that all phonon frequencies are real (indicating no instabilities) for lattice constants within $\pm 2\%$ of the experimental value (a_0=3.851 Å). Also, the choice of U does not significantly alter the phonon dispersions.

We now discuss how appropriate choice of the antiferrodistortive octahedral rotations in the substrate may be used to activate particular latent lattice instabilities in a functional thin film. As we showed earlier, if the octahedral tilt pattern in the film can be modified, it may be possible to switch between the types of electronically-driven structural instabilities that couple to the rotational modes.

This is shown schematically in Fig. 4 for the $(SrTiO_3)_n/(SrFeO_3)_1$ superlattices. When the superlattice exhibits the orthorhombic *Pnma* octahedral tilt pattern $a^-a^-c^+$, the Jahn-Teller distortion is activated due to the orbital degeneracy in the highly confined $SrFeO_3$ layers. On the other hand, the $a^0a^0c^-$ tilt pattern is found to occur with the octahedral breathing distortion.[32] The actual ground state obtained experimentally will likely be determined by the octahedral structural distortions, since these often condense at higher temperatures than the electronic instabilities. Therefore selection of a substrate with octahedral rotations compatible with the symmetry of a certain electronic instability will dictate which phase is observed. The presence (or absence) of octahedral rotations in a substrate is thus critical to determining the orbitally or charge-ordered electronic configurations in the ferrate/titanate superlattices.

We now address how to experimentally enhance the penetration length of the coherency-induced octahedral rotation proximity effect in thin film perovskites. The first critical aspect is in the selection of the substrate: A larger proximity effect can be obtained by choosing substrates which show in-plane ($a^\pm a^\pm c^\pm$) tilts with *Pnma* (orthorhombic) or $C2/c$ (monoclinic or pseudorhombohedral) space groups rather than only out-of-plane, $a^0a^0c^\pm$ octahedral rotation patterns: The long-range correlations of the in-plane tilt patterns along the out-of-plane direction should force the rotations of successive octahedra in planes perpendicular to the rotation axis; this will in turn yield larger penetration depths across the interface. Here, lanthanide-based scandate substrates are ideal candidates due to their large octahedral rotation angles; they also allow fine tuning of the *Pnma* $a^-a^-c^+$ rotation angles by solid-solution alloying. While measurable changes in rotation angles ($<1°$) have recently been reported with x-ray diffraction[13] and Z-contrast electron microscopy techniques[25] on $SrTiO_3$ and $LaAlO_3$ substrates, the longer in-plane coherence length from such substrates could eventually make characterization of the proximity effect routine.

Alternatively, thin film growth on various substrate orientations or with minor changes in the substrate vicinal cut could be used to control the types of octahedral rotational antiphase domain boundaries induced by the substrate. The second aspect which dictates the size of the proximity effect is the susceptibility of the film to octahedral rotations. Here, bulk perovskite oxides which have soft lattice modes (or latent lattice/electronic instabilities), while also exhibiting stiff transition metal–oxygen bonds are the best choices: These characteristics encourage lattice strain accommodation by rotation of nearly rigid octahedra, rather than by rumpling of interface atomic layers.

In summary, we used density functional calculations and the model $SrFeO_3/SrTiO_3$ superlattice system to show that thin film perovskite heterointerfaces are not only sensitive to the elastic strain at the interface, but also to the octahedral rotation patterns present in the substrate. We found that the $a^0a^0c^-$ tilt pattern in the $SrTiO_3$ substrate propagates into the $SrFeO_3$ film interfacial layers. Interestingly, we find that the substrate not only affects the rotation patterns of the film, but that the entire heterostructure can adopt a tilt pattern that is absent in the parent substrate and film phase diagrams. Our findings may partly explain the recent anomalous structural phase transitions observed in $SrTiO_3$ substrates used to support manganite/cuprate superlattices,[4] as well as the reported resonant phonon coupling[26] in $SrTiO_3/La_{1-x}Sr_xMnO_3$ superlattices. We described how the ability to control the octahedral rotation textures present in thin films with the substrate proximity effects affords an additional parameter for tuning the atomic and electronic structure of orbitally degenerate perovskite oxides. The challenge remains, however, to develop an intuition for rational materials design based on octahedral texturing; we encourage further experimental study of substrate proximity effects on the octahedral rotations and the subsequent changes in the electronic structure of thin film perovskites.

This work was supported by NDSEG-DoD (J.M.R.) and the NSF through Grant No. DMR 0940420 (N.A.S.). We thank S. May, C. Adamo, and D. Schlom for useful discussions.

*Author to whom correspondence should be addressed: rondinelli@anl.gov

†Present address: X-ray Science Division, Argonne National Laboratory, Argonne, Illinois 60439 USA.

[1] D. G. Schlom *et al.*, Annu. Rev. Mater. Res. **37**, 589 (2007).
[2] F. He, B. O. Wells, Z. G. Ban, S. P. Alpay, S. Grenier, S. M. Shapiro, W. Si, A. Clark, and X. X. Xi, Phys. Rev. B **70**, 235405 (2004).
[3] C. K. Xie *et al.*, Appl. Phys. Lett. **93**, 182507 (2008).
[4] J. Hoppler, J. Stahn, H. Bouyanfif, V. K. Malik, B. D. Patterson, P. R. Willmott, G. Cristiani, H. U. Habermeier, and C. Bernhard, Phys. Rev. B **78**, 134111 (2008).
[5] R. Loetzsch *et al.*., Appl. Phys. Lett. **96**, 071901 (2010).
[6] S. Okamoto, A. J. Millis, and N. A. Spaldin, Phys. Rev. Lett. **97**, 056802 (2006).
[7] D. I. Bilc and D. J. Singh, Phys. Rev. Lett. **96**, 147602 (2006).
[8] J. M. Rondinelli, A. S. Eidelson, and N. A. Spaldin, Phys. Rev. B **79**, 205119 (2009).
[9] E. Bousquet *et al.*, Nature (London) **452**, 732 (2008).
[10] R. J. Zeches *et al.*, Science **326**, 977 (2009).
[11] J. He *et al.*, arXiv:1006.5758 (unpublished).
[12] C. L. Jia, S. B. Mi, M. Faley, U. Poppe, J. Schubert, and K. Urban, Phys. Rev. B **79**, 081405 (2009).
[13] S. J. May, *et al.*, Phys. Rev. B **82**, 014110 (2010).
[14] J. B. MacChesney *et al.*, J. Chem. Phys. **43**, 1907 (1965).
[15] W. Jauch and A. Palmer, Phys. Rev. B **60**, 2961 (1999).
[16] G. Kresse and J. Furthmuller, Phys. Rev. B **54**, 11169 (1996).
[17] G. Kresse and D. Joubert, Phys. Rev. B **59**, 1758 (1999).
[18] S. L. Dudarev, G. A. Botton, S. Y. Savrasov, C. J. Humphreys, and A. P. Sutton, Phys. Rev. B **57**, 1505 (1998).
[19] I. Shein *et al.*, Phys. Solid State **47**, 2082 (2005).
[20] J. M. Rondinelli and N. A. Spaldin, Phys. Rev. B **81**, 085109 (2010).
[21] H. Unoki *et al.*, J. Phys. Soc. Jpn. **23**, 546 (1967).
[22] N. Sai and D. Vanderbilt, Phys. Rev. B **62**, 13942 (2000).
[23] C.-H. Lin *et al.*, J. Appl. Phys. **100**, 084104 (2006).
[24] A. J. Hatt *et al.*, arXiv:0808.3792 (unpublished).
[25] A. Borisevich *et al.*, Phys. Rev. Lett. **105**, 087204 (2010).
[26] Y. Segal *et al.*, APS Meeting Abstracts pp. 37004–+ (2010).
[27] E. Courtens, Phys. Rev. Lett. **29**, 1380 (1972).
[28] P. Woodward, Acta Crystallogr., Sect. B: Struct. Sci. **53**, 44 (1997).
[29] T. Mizokawa, D. I. Khomskii, and G. A. Sawatzky, Phys. Rev. B **60**, 7309 (1999).
[30] We note that there is an overestimate in our LDA calculation of the bulk rotation angle of θ=5.7° compared to the experimental value of θ=2.1° (Ref. 27). Previous work indicates that working at the experimental volume does not dramatically improve the calculated value since the inconsistency originates from quantum point fluctuations that are not captured by the exchange-correlation functionals available to DFT (Ref. 22).
[31] The weak dependence on strain is likely due to the rectangular planar oxygen coordination of Sr: less energy stabilization is obtained from the strain-induced covalency modifications than the elastic energy gain available in the distorted tetragonal coordination found in the $a^0a^0c^-$ tilt pattern (Ref. 28).
[32] Coupling of this type is found in isoelectronic d^4 $LaMnO_3$, where the orthorhombic $a^-a^-c^+$ tilt pattern combines with a long-range ordering of Jahn-Teller distortions, in preference to the breathing distortion (Ref. 29).